ACS Macro Letters

Letter

pubs.acs.org/macroletters

Entropic Mechanism for the Lower Critical Solution Temperature of Poly(ethylene oxide) in a Room Temperature Ionic Liquid

Eunsong Choi[†] and Arun Yethiraj*[,‡]

Departments of [†]Physics and [‡]Chemistry, University of Wisconsin, Madison, Wisconsin 53706, United States

ABSTRACT: Polymers exhibit interesting phase behavior in room temperature ionic liquids. For example poly(ethylene oxide) (PEO) displays a lower critical solution temperature (LCST) in [BMIM]-[BF_4] with a critical temperature and concentration that are only weakly dependent on molecular weight, contrary to the behavior of polymers in other solvents. To shed light on the mechanism of the LCST, we study the phase behavior of PEO in [BMIM][BF_4] using molecular dynamics (MD) simulations. The simulations show the signature of a phase transition as the temperature is increased. At low temperatures, interactions similar to a hydrogen bond are found between the imidazolium hydrogen and the PEO oxygen (HI−O H-bond) and the imidazolium hydrogen and the anion fluorines (HI−F H-bond). These interactions stabilize the mixed phase. A potential of mean force (PMF) analysis shows an entropic cost associated with the HI−O H-bond, which makes the bond formation unfavorable at higher temperatures, while the HI−F H-bond does not show a significant temperature dependence: This suggests that LCST phase separation is driven by the entropic penalty of the polymer for a PEO-cation hydrogen bond. We test the effect of scaling the charges on the [BMIM][BF_4]. Interestingly, the scaled charge force-field does not predict a phase separation at any temperature, thus, emphasizing the pitfalls of charge scaling for mixtures.

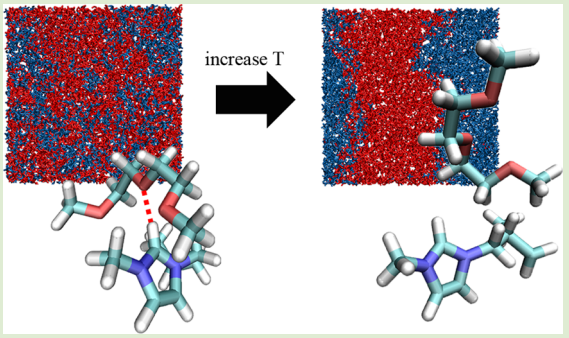

Ionic liquids have attracted great attention in the past decade due to their interesting unique properties, such as negligible vapor pressure, high thermal and chemical stability, relatively high ionic conductivity, and nonflammability. These properties have made them an excellent candidate for the next generation solvents that could potentially replace traditional organic solvents in many areas. When mixed with certain polymers, ionic liquids have potential in materials design because the polymers can provide mechanical integrity and structural persistence that ionic liquids lack.[1] These include applications as membranes for fuel cells, polymerized ion gels for gas separation, basis of electromechanical actuators, and electrolytes in lithium batteries. Understanding the phase behavior and miscibility of polymers in ionic liquids is therefore crucial for materials design. There is also fundamental interest because the phase behavior is unusual. Poly(ethylene oxide) (PEO) displays a lower critical solution temperature (LCST) in 1-ethyl-3-methylimidazolium tetrafluoroborate ([EMIM][BF_4]) and 1-butyl-3-methylimidazolium tetrafluoroborate ([BMIM][BF_4]). Interestingly, unlike typical polymer solutions, the critical composition occurs at high polymer concentrations, and the critical temperature is insensitive to polymer molecular weight.[2,3] In this work, we use atomistic computer simulations to study the phase behavior of PEO in [BMIM][BF_4] .

An LCST usually occurs when both enthalpy of mixing and entropy of mixing are negative. The negative entropy of mixing is often explained either by specific interactions[4−6] or compressibility effects.[7,8] For PEO in water it is argued that the system is mixed at low temperatures because of hydrogen bonds between the polymer and solvent,[5,6] with an entropic cost due to solvent−polymer versus solvent−solvent hydrogen bonds. At high temperatures, the entropic effect dominates and the system phase separates, while at low temperatures the energetic effect dominates and the system is mixed.

The mechanism of the LCST for PEO in ionic liquids, however, is not well understood. Recently, White and Lipson showed that they can reproduce the LCST phase diagram of PEO/IL system using a compressible lattice model.[9] They argued that polymer-rich critical composition is caused by the significantly weaker pure solute cohesive energy (compared to that of the solvent), and nano scale aggregation of the ionic liquids.

A number of experimental studies emphasize the importance of hydrogen bonding on the phase behavior. (1) Lee et al.[3] showed that replacing the imidazolium hydrogen with a methyl group changes the shape of phase diagram quite significantly, thus emphasizing the importance of the hydrogen bonds between H atom of the imidazolium ring and O atom of PEO for the phase behavior. (2) Tsuda et al.[10] carried out ^{1}H NMR spectroscopy measurements for a PEO derivative, poly(ethyl glycidyl ether) (PEGE), in 1-ethyl-3-methylimidzolium bis-(trifluoromethane sulfonyl)amide ([EMIM][NTf_2]), and reported a down shift in NMR signals as the concentration of PEGE increased, possibly reflecting increased hydrogen bonds

Received: May 29, 2015
Accepted: July 10, 2015
Published: July 13, 2015

DOI: 10.1021/acsmacrolett.5b00355
ACS Macro Lett. 2015, 4, 799−803

Table 1. Comparison of Predictions for Physical Properties of [BMIM][BF_4] at 300 and 400 K from the Full Charge (Q1) and Scaled Charge (Q084) Force-Fields

	T (K)	ρ (kg/m^3)	ΔH (kJ mol^{-1})	D_+ (10^{-11} m^2 s^{-1})	D_- (10^{-11} m^2 s^{-1})
MD (Q1)	300	1176	188	0.13	0.06
MD (Q084)	300	1141	148	2.0	1.2
Exp	300	1202[17]	128[a,18]	1.60[17]	1.49[17]
MD (Q1)	400	1109	178	8.89	6.38
MD (Q084)	400	1059	140	31.83	20.94
Exp	400	1130[17]		27.5[17]	31.5[17]

[a]Estimated using the empirical correlation with the surface tension at T = 298 K.

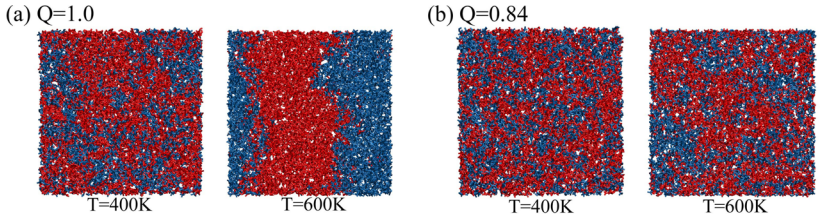

Figure 1. Snapshots of PEO (red) in [BMIM][BF_4] (blue) at two different temperatures, 400 and 600 K. (a) Full charge OPLS-AA force field, and (b) Scaled charge (Q = 0.84) force field.

in the PEGE/[EMIM][NTf_2] system. (3) Li and Wu[11] found, using various spectrosopy techniques, that there are four types of hydrogen bonds in the PEO/[EMIM][BF_4] system: namely, HI−O (type I), H(PEO)−F (type II), HI−F (type III), and OH(PEO)−F (type IV). By observing the temperature dependence of the corresponding peaks in the spectra, they argued that phase separation is driven mainly by the disruption of HI−O hydrogen bonds. However, their observation does not address the question of what makes the HI−O hydrogen bonds behave differently from the other competing interactions such as the HI−F bonds, that have an opposite role on mixing.

In this work, we study the phase behavior of PEO in [BMIM][BF_4] using molecular dynamics (MD) simulations. The simulations predict phase separation upon heating, in qualitative agreement with the experiments. Based on the spatial distribution and the potential of mean force (PMF) analysis, we show that there are two hydrogen bond like associations: HI−O and HI−F where only the former comes with a significant entropic cost that is associated with the local arrangement of PEO near the BMIM cation. We argue that the temperature sensitive competition between the two types of hydrogen bonds drives the phase behavior of this system. We also study the effect of charge scaling on the phase behavior. Interestingly, the scaled charge model does not show any phase separation for temperatures as high as 700 K. We show that mixing at high temperature in the charge scaled force-field is driven by reduced solvent−solvent interaction that breaks the subtle balance between different components in the original force-field, reflecting the pitfalls of charge scaling.

We investigate two force fields for PEO in [BMIM][BF_4]; the OPLS-AA force-field,[12,13] which has a charge of Q = 1 on the cation (and $-Q$ on the anion), and the scaled-charge OPLS-AA force-field,[14] where Q = 0.84. All the other interactions are the same in the two models. We refer to these force-fields as the Q1 and Q084 force-fields These force-fields are in good agreement with experiment for the density and heat of vaporization of [BMIM][BF_4] when compared to experiment (see Table 1). Overall, the scaled-charge model is significantly more accurate, especially for the diffusion constants. Our observations are in line with previous studies[14−16] and shows that the charge scaling, indeed, effectively improves predictions for the bulk ionic liquids properties.

The full charge OPLS-AA force-field shows a phase transition when the temperature is increased, consistent with experiment, but the scaled-charge force-field does not. The snapshot in Figure 1a shows that a clear phase separation is observed with the OLPS-AA force-field at 600 K. (In the figure, the atoms of the PEO are colored red and the atoms of the ionic liquid are colored blue.) The phase transition occurs at a temperature near 500 K, but it is hard to estimate the transition temperature accurately with MD simulations. The scaled charge force-field, however, qualitatively fails when the phase behavior of PEO/[BMIM][BF_4] solution is concerned. Figure 1b shows that the scaled charge, Q084 model does not show phase separation at all, even up to 700 K.

The superior performance of the Q084 force field for the bulk ionic liquid does not carry over to mixtures, where we find that it is in qualitative disagreement with experiment. We suggest that this is because it significantly underestimates the magnitude of the cohesive energy density of the ionic liquid. Although this does not affect the density or heat of vaporization, and improves predictions for the diffusion coefficients, it has a dramatic effect on the phase behavior. This can be reconciled by noting that the density and diffusion coefficients are sensitive to the short-ranged part of the interaction while the cohesive energy density is sensitive to the interaction potential on all length-scales. The heat of vaporization is sensitive to interactions on all length-scales as well, but benefits from a cancellation of gas phase and liquid phase contributions.

An investigation of hydrogen bonding provides insight into the phase behavior. Figure 2 depicts the spatial distribution of three hydrogen bonds (for the Q1 model) at temperatures below and above the LCST. At low temperatures there is strong hydrogen bonding between the imidazolium C_2 hydrogen and the PEO oxygen atoms, near r = 0.2 nm and ϕ = 0−1 radians. (Similar behavior is observed for the C_4 and C_5 hydrogen atoms.) The interaction between the PEO hydrogen and the anion is relatively week. These hydrogen bond like associations

DOI: 10.1021/acsmacrolett.5b00355
ACS Macro Lett. 2015, 4, 799−803

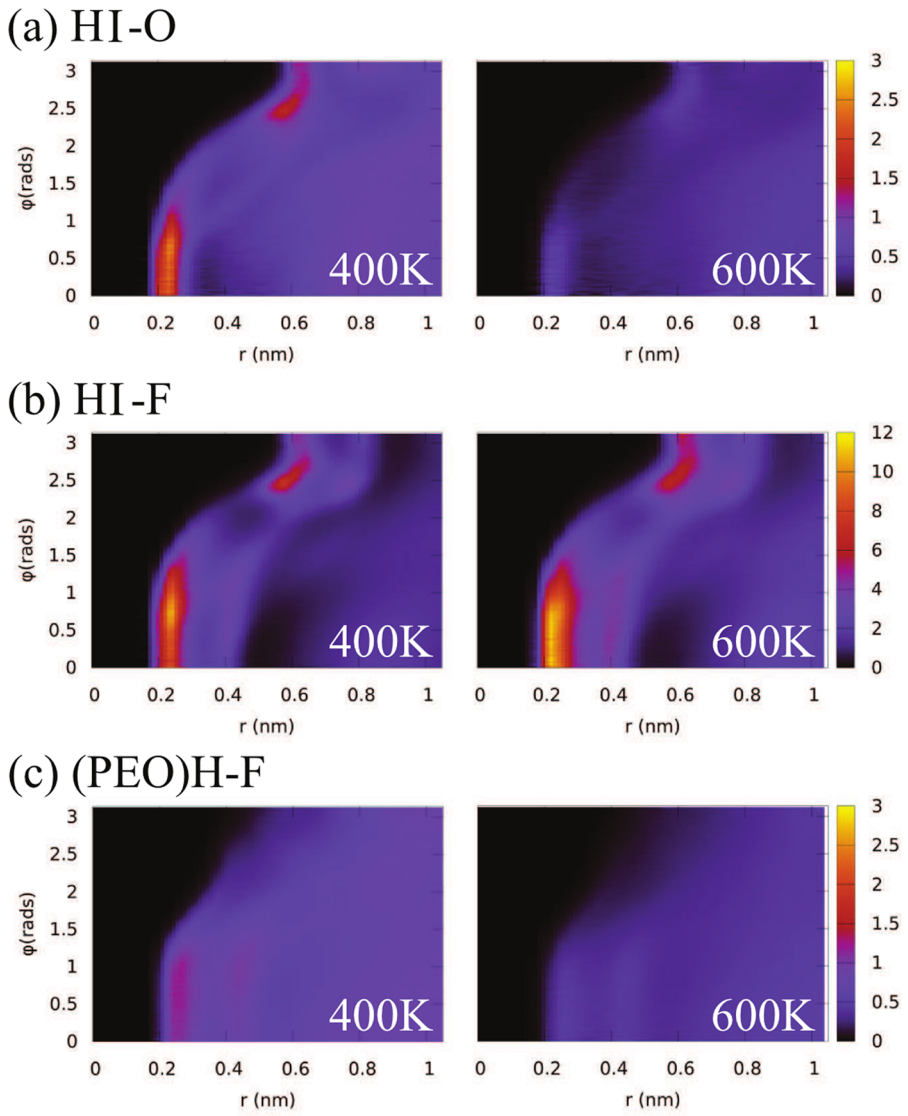

Figure 2. Spatial distribution functions for hydrogen bonding interactions at T = 400 K (left) and T = 600 K (right). The distance r is measured between the hydrogen-bonding moieties, and the angle ϕ is measured between this vector and the C−H bond. The panels are for (a) imidazolium C_2 hydrogen and PEO oxygen, (b) imidazolium C_2 hydrogen and fluorine, and (c) PEO hydrogen and fluorine. The figures show the formation of hydrogen bond-like interactions between imidazolium hydrogens and PEO oxygens, and imidazolium hydrogens and fluorines: the former gets disrupted at higher temperature, but the latter does not. The association between the PEO hydrogens and anion fluorines are weak. The hydrogen bonding behavior of the imidazolium C_4 and C_5 hydrogens is similar to that of the C_2 hydrogen in parts (a) and (b).

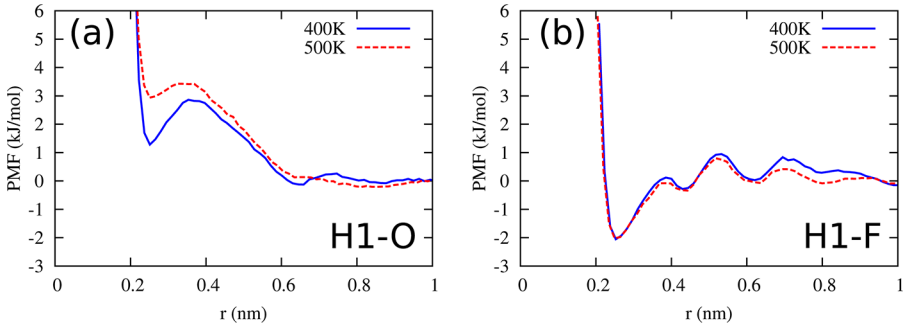

Figure 3. Potential of mean force (PMF) calculation between (a) oxygen of PEO and hydrogen of imidazolium ring and (b) fluorine of $[BF_4]^-$ and hydrogen of imidazolium ring at two different temperatures.

are driven by charge−dipole interaction between two groups. At the higher temperature the two hydrogen bonds behave quite differently; while the HI−O assocations are almost suppressed, the HI−F associations are unaffected or even stronger. This observation is in agreement with the recent spectroscopy measurement by Li et al.[11] in which showed that

DOI: 10.1021/acsmacrolett.5b00355
ACS Macro Lett. 2015, 4, 799−803

the HI−O hydrogen bonds get disrupted at higher temperatures.

Potential of mean force calculations show that the HI−O hydrogen bond comes with an entropic cost, but the HI−F does not. Figure 3 shows the PMF between (a) imidazolium C_2 hydrogen and PEO oxygen, and (b) imidazolium C_2 hydrogen and fluorine of BF_4^-, at 400 and 500 K. At 400 K both PMF plots clear a minimum near r = 0.2 nm, consistent with the spatial distribution function in Figure 2. At the higher temperature, however, the minimum in the HI−O PMF is much shallower, but the HI−F PMF is essentially the same as at 400 K. This implies that there is a strong entropic contribution to the minimum in the HI−O PMF while the HI−F PMF is essentially energetic in nature.

We hypothesize that the formation of HI−O hydrogen bond restricts the local conformation of PEO due to steric hindrance between adjacent CH_2 groups of PEO and the imidazolium ring, and hence decreases entropy. In contrast, the HI−F association does not involve significant local arrangement, and is thus relatively insensitive to temperature. To estimate this we introduce a bond between the PEO oxygen atom and the imidazolium hydrogen and show that this restricts the conformations available. If a sphere were attached it would still be able to rotate freely around the cation, but the polymeric nature of PEO can prevent the accessible region of space. Figure 4 supports this hypothesis; when the central oxygen is bound to the imidazolium C_2 hydrogen via a harmonic potential, the neighboring oxygen atoms are mostly restricted to the direction facing the plane of the imidazolium ring.

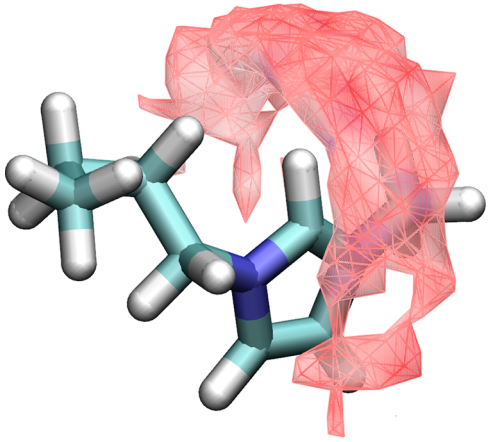

Figure 4. Probability isosurface plot of three adjacent oxygen atoms of PEO when the central oxygen is bound to the imidazolium hydrogen via harmonic spring. The figure suggests that the local conformation of PEO chain is restricted to a particular orientation, when PEO oxygen and imidazolium hydrogen form a hydrogen bond, due to steric hindrance between adjacent CH_2 groups of PEO and methyl and CH_2 groups of BMIM.

We attribute the failure of the Q084 force-field to predict a phase transition to a significant under-estimation of the energy of mixing compared to the Q1 force-field. At sufficiently high temperatures, the configurational entropy of mixing is positive and the system is mixed. As the temperature is lowered, the positive energy of mixing causes a phase separation in the Q1 force-field (at temperatures higher than studied in this work). This phase separation is not seen in the Q084 force-field because charge scaling results in a significantly lower energy of mixing. Figure 5 shows computed ΔE_{mix} and its decomposition.

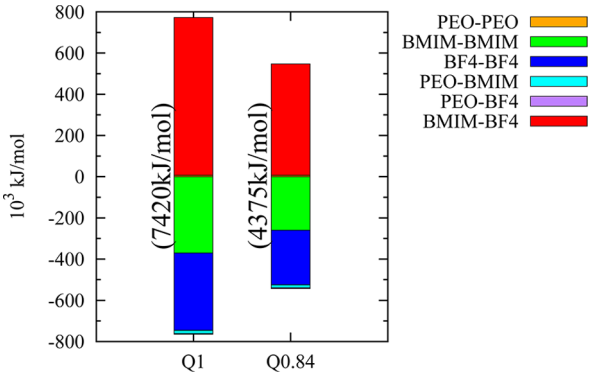

Figure 5. Total energy of mixing and decomposed contributions at 600 K computed by using the demixed state trajectory (Q = 1.0 force-field) and the mixed state trajectory (Q = 0.84 force-field). The phase mixing in the scaled charge force-field is driven by reduced BMIM-BF4 interactions that are most greatly affected by charge scaling (proportional to Q^2).

The total energy of mixing is positive for both force-fields but much larger in the Q1 force-field. In the Q084 force-field the phase transition does not occur because of much reduced solvent−solvent interactions, and the system is mixed at all temperatures. The system becomes mixed again in the Q1 force-field at lower temperatures because of the decreased energy of mixing from the polymer-cation hydrogen bond, when the temperature is low enough that the entropic cost of this bond is not important.

In summary, we have carried out MD simulations on the phase behavior of PEO in [BMIM][BF_4]. Based on the spatial distribution and the PMF analysis for strongly associating groups, we find two types of hydrogen bond like interactions, between the imidazoiium (C_2, C_4, and C_5) hydrogen and the PEO oxygen (HI−O) and anion fluorines (HI−F) hydrogen bonds. We find that the HI−O hydrogen bonds get disrupted at higher temperature, thus driving the phase separation. This is in agreement with the recent spectroscopy measurements.[11] The difference between the two types of associations is that, while the HI−O hydrogen bond is entropically strongly repulsive, the HI−F hydrogen bond has negligible entropic cost. We show that this entropic cost is associated with a particular local arrangement of PEO near BMIM required to reduce steric hindrance. The study supports the experimental observations that the HI−O H-bonds drive the LCST phase behavior[2,3] and provides a mechanism in terms of polymer conformational entropy for the entropic cost associated with this hydrogen bond.

The phase behavior is sensitive to the force-field. A popular scaled charge force-field does not show any phase transition at all, which we attribute to a disruption of the balance between entropy and energy when the charges on the ionic liquid are scaled down. The scaled-charge force-field is accurate for the bulk ionic liquid but not when a solute is introduced, thus, emphasizing the pitfalls of ad hoc charge-scaling.

METHODS

All simulations are carried out using the OPLS-AA force-field[12,13] and Gromacs version 4.6.5.[19] In the molecular dynamics simulations 55 chains of PEO40 and 442 [BMIM][BF_4] pairs are simulated at four different temperatures, 400, 500, 600, and 700 K, using both full charge (Q1) and scaled charge (Q084) force-fields. All simulated systems are first equilibrated for 2 ns with a time step of 2 fs using Nosé−Hoover thermostat[20,21] and Berendsen barostat.[22] The

DOI: 10.1021/acsmacrolett.5b00355
ACS Macro Lett. 2015, 4, 799−803

production run is carried out in NVT ensemble using Nosé−Hoover thermostat. The potential of mean force (PMF) is computed using Umbrella sampling technique followed by the weighted histogram analysis method (WHAM).[23] For the HI−O association, a single PEO2 chain and 200 [BMIM][BF_4] ion pairs are used. The oxygen atom of the central monomer of PEO2 and an imidazolium hydrogen is constrained using harmonic potentials centered at 25 different distances that are 0.25 nm apart, between 0.18 and 1.18 nm. Each simulation is carried out for 40 ns. For the HI−F association, 200 [BMIM][BF_4] ion pairs are simulated with an imidazolium hydrogen and a fluorine being constrained using the same harmonic potentials. For all simulations, the Lennard-Jones potentials are shifted to zero at 1.4 nm, and for long-ranged electrostatic interactions, the Particle-Mesh-Ewald(PME) method[24,25] with a spacing of 0.12 nm and a real space cutoff distance 1.4 nm is used.

AUTHOR INFORMATION

Corresponding Author

*Tel.: 608-262-0258. E-mail: yethiraj@chem.wisc.edu.

Notes

The authors declare no competing financial interest.

ACKNOWLEDGMENTS

This work was partially supported by the National Science Foundation under Grant No. CHE-1111835. We are grateful for generous computational support from gordon machine in the San Diego Supercomputer Center(SDSC) under Grant No. TG-CHE090065 and the UW Madison Chemistry Department cluster Phoenix under Grant No. CHE-0840494 and compute resources and assistance of the UW-Madison Center for High Throughput Computing (CHTC).

REFERENCES

(1) Lodge, T. P. *Science* **2008**, *321*, 50−51.
(2) Lee, H.-N.; Lodge, T. P. *J. Phys. Chem. Lett.* **2010**, *1*, 1962−1966.
(3) Lee, H.-N.; Newell, N.; Bai, Z.; Lodge, T. P. *Macromolecules* **2012**, *45*, 3627−3633.
(4) ten Brinke, G.; Karasz, F. E. *Macromolecules* **1984**, *17*, 815−820.
(5) Dormidontova, E. *Macromolecules* **2004**, *37*, 7747−7761.
(6) Dormidontova, E. *Macromolecules* **2002**, *35*, 987−1001.
(7) Lacombe, R. H.; Sanchez, I. C. *J. Phys. Chem.* **1976**, *80*, 2568−2580.
(8) Sanchez, I. C.; Lacombe, R. H. *Macromolecules* **1978**, *11*, 1145−1156.
(9) White, R. P.; Lipson, J. E. G. *Macromolecules* **2013**, *46*, 5714−5723.
(10) Tsuda, R.; Kodama, K.; Ueki, T.; Kokubo, H.; Imabayashi, S.-i.; Watanabe, M. *Chem. Commun.* **2008**, 4939−4941.
(11) Li, W.; Wu, P. *Soft Matter* **2013**, *9*, 11585−11597.
(12) Sambasivarao, S. V.; Acevedo, O. *J. Chem. Theory Comput.* **2009**, *5*, 1038−1050.
(13) Mondal, J.; Choi, E.; Yethiraj, A. *Macromolecules* **2014**, *47*, 438−446.
(14) Chaban, V. V.; Voroshylova, I. V.; Kalugin, O. N. *Phys. Chem. Chem. Phys.* **2011**, *13*, 7910−7920.
(15) Youngs, T. G. A.; Hardacre, C. *ChemPhysChem* **2008**, *9*, 1548−1558.
(16) Bhargava, B. L.; Balasubramanian, S. *J. Chem. Phys.* **2007**, *127*, 114510.
(17) Tokuda, H.; Hayamizu, K.; Ishii, K.; Abu bin Hasan Susan, M.; Watanabe, M. *J. Phys. Chem. B* **2004**, *108*, 16593−16600.
(18) Verevkin, S. P. *Angew. Chem., Int. Ed.* **2008**, *47*, 5071−5074.
(19) Pronk, S.; Pall, S.; Schulz, R.; Larsson, P.; Bjelkmar, P.; Apostolov, R.; Shirts, M. R.; Smith, J. C.; Kasson, P. M.; van der Spoel, D.; Hess, B.; Lindahl, E. *Bioinformatics* **2013**, *29*, 845−854.
(20) Nosé, S. *Mol. Phys.* **1984**, *52*, 255−268.
(21) Hoover, W. *Phys. Rev. A: At., Mol., Opt. Phys.* **1985**, *31*, 1695−1697.
(22) Berendsen, H. J. C.; Postma, J. P. M.; van Gunsteren, W. F.; DiNola, A.; Haak, J. R. *J. Chem. Phys.* **1984**, *81*, 3684−3690.
(23) Kumar, S.; Bouzida, D.; Swendsen, R. H.; Kollman, P. A.; Rosenberg, J. M. *J. Comput. Chem.* **1992**, *13*, 1011−1021.
(24) Darden, T.; York, D.; Pederson, L. G. *J. Chem. Phys.* **1993**, *98*, 10089.
(25) Essmann, U.; Perera, L.; Berkowitz, M. L.; Darden, T.; Lee, H.; Pederson, L. G. *J. Chem. Phys.* **1995**, *103*, 8577.

DOI: 10.1021/acsmacrolett.5b00355
ACS Macro Lett. 2015, 4, 799−803